The International Society for Optical Engineering

HOLOGRAPHY

Combining optical holograms with interactive computer graphics

Holography and computer graphics are used as tools to solve individual research, engineering, and presentation problems within several domains. Up until now, however, these tools have been applied separately. Our intention is to combine the technologies to create a powerful tool for science, industry, and education (see website for project details).

We use video projectors instead of analog light bulbs, the main advantage of which is that the wave used to reconstruct a white-light hologram can be digitized. Thus it is possible to control the amplitude and wavelength of each discrete portion of the wavefront over time.[1] Today's computer graphics capabilities allow the merging of any kind of two- or three-dimensional graphical elements seamlessly with the recorded holographic content. Their integration with holography has the potential, therefore, to lead to efficient visualization tools that combine the advantages of holography and computer graphics.

It is possible to reconstruct the object wave of a hologram only partially, leaving gaps where graphical elements can be inserted. Both reflection holograms (without an opaque backing layer) and transmission holograms remain transparent if not illuminated. Thus,

Continues on page 9.

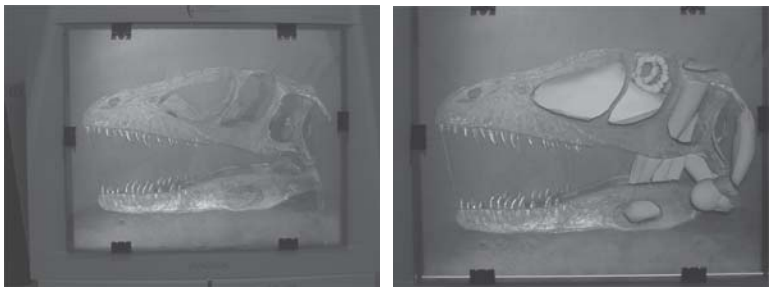

Figure 1. Rainbow hologram of a dinosaur skull combined with graphical representations of soft tissue and bones.

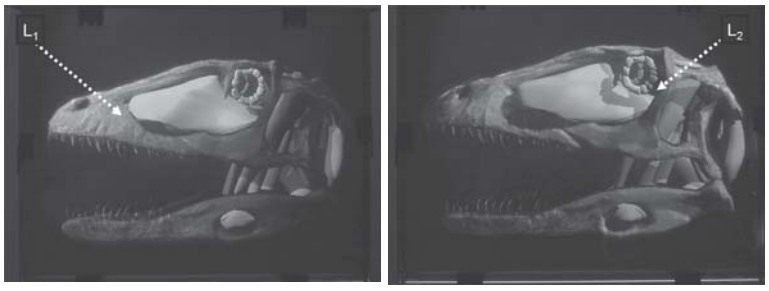

Figure 2. A rainbow hologram with 3D graphical elements and synthetic shading and shadow effects.

Calendar—*See page 7.*

Technical Group Registration Form—*See page 11.*

Newsletter now available on-line

Technical Group members are being offered the option of receiving the Holography Newsletter electronically. An e-mail is being sent to all group members with the web location for this issue, and asking members to choose between the electronic and printed version for future issues. If you are a member and have not yet received this message, then SPIE does not have your correct e-mail address.

To receive future issues elec-tronically, please send your e-mail address to:

spie-membership@spie.org

with the word holography in the subject line of the message and the words **electronic version** in the body of the message.

If you prefer to receive the newsletter in the printed format, but want to send your correct e-mail address for our database, include the words **print version preferred** in the body of your message.

An update on silver halide holographic materials

Holographic materials have constantly improved over the past few years. In order to provide potential users with up-to-date information about speed, absorption, maximum diffraction efficiency and reconstruction bandwidth, we conducted a comparison of different holographic materials that were on the market in 2004. We investigated the silver halide materials from ColourHolographic Ltd. (BB-450, BB-520, BB-640), Yves Gentet[1] (Ultimate-08, Ultimate-15), and GEOLA[2] (VRP-M, PFG-01, PFG-3C). The purpose of our evaluation was to choose one of the materials for the work in our laboratory. Though such investigations have been conducted before,[3-6] an update of the latest material characteristics seemed to be necessary.

Evaluation procedure

We recorded plane-wave reflection holograms in all silver halide emulsions by means of a stepper-motor-driven computer-controlled exposure stage. To cover a large range of possible applications, different laser wavelengths were used: these included several argon laser lines, HeNe lasers at 633nm, and pulsed frequency-doubled Nd:YAG lasers at 532nm. We developed and bleached the emulsions as suggested by the manufacturers and evaluated the reflection holograms with a fibre spectrometer.

We recorded fringes with a high spatial frequency in order to verify the material resolutions specified by the manufacturers. The reference beam was incident from 45° and the object beam was set to an angle of 0° in a reflection geometry, yielding an interbeam angle of $\Delta\Theta = 135°$. Both beams were s-polarized and the beam ratio K was constant at

$$\lambda_{ref}/\lambda_{obj} = K = 1$$

For every examined combination of material and wavelength, over one hundred single holograms were recorded with varying exposure times. For evaluation, a fibre-coupled collimated tungsten light source was used. The zero-order light that was transmitted through the hologram was coupled into another fibre and examined with a spectrometer. A typical transmission spectrum from a recorded hologram is shown in Figure 1.

Material properties

Our main interest was focused on the maximum-achievable diffraction efficiency and the bandwidth of the silver-halide emulsions. These two parameters are essential for holographic materials, since they determine how much light can effectively be used for reconstruction. We further investigated the shrinkage of the emulsion and losses due to absorption and scattering. Detailed curves for all parameters, for large exposure ranges and for up to five laser wavelengths, are also available on request. Due to the restricted space, Table 1 gives a short summary of the main results for the case of recording at 633nm.

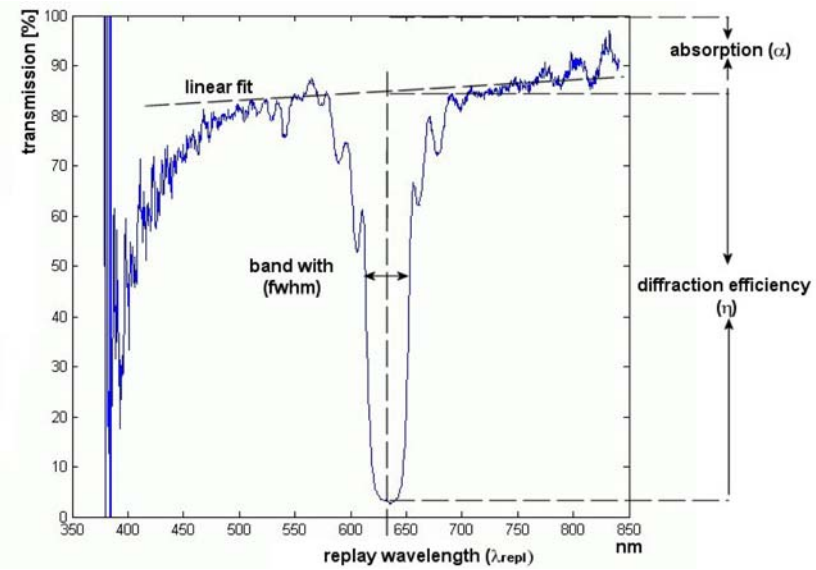

Figure 1. Transmission spectrum of a typical hologram.

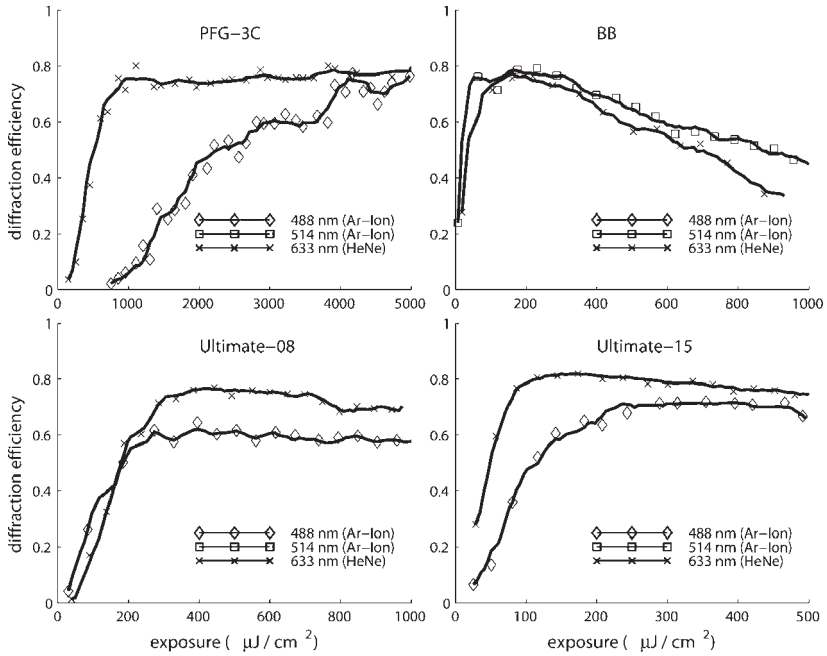

Figure 2. Diffraction efficiencies of the holographic materials under investigation.

Results

Figure 2 shows the diffraction efficiency for most of the materials under investigation (VRP-M and PFG-01 are not displayed here) versus the exposure dose. Basically all materials were able to achieve around 80% diffraction efficiency at their optimal exposure. Furthermore, we could deduce several facts besides the optimal exposure range for the holographic materials. First, basically all materials are capable of replaying near the recording wavelength if the recommended development

Continues on page 10.

Controlling phase and amplitude image reconstructions in digital holography: achievements and perspectives

The idea of using a computer to reconstruct a hologram[1] was proposed for the first time by Goodman and Laurence and by Kronrod *et al*..[2] The development of computer technology and solid-state image sensors then made it possible to directly record holograms using a charge-coupled-device (CCD) camera.[3] This important step is commonly referred to as digital holography (DH), where the amplitude and phase of the object beam can be extracted separately through the complex wavefront. The numerical reconstruction procedure is based either on the calculation of the diffraction integral via a Fresnel-transformation method (FTM) or a convolution method.

In the FTM, the phase- and amplitude-image reconstruction pixel (RP) size (Δx) depends on the wavelength λ used via the relation:

$$\Delta x = d\lambda / N\Delta\xi$$

Here d is the reconstruction distance—the distance measured backward from the hologram plane ($\xi - \eta$) to the image plane (x - y)—and N^2 is the number of pixels of size $\Delta\xi$ in the CCD array (a square array is considered here). We have investigated theoretically[4,5] a simple numerical procedure for controlling the numerical reconstruction using the FTM, and demonstrated experimentally its use in DH microscopy (DHM) for micro-electro-mechanical-systems (MEMS) investigation.

Figure 1 shows an application DHM for a quasi-real-time inspection of a silicon cantilever (50μm×50μm). The recording set up consists basically of a Mach-Zehnder interferometer for reflection imaging at wavelength 532nm. The sample was heated to the temperature range 23-123°C, using a remote-controlled element. While heating the sample, the phase-shift of the interference fringes was detected in quasi-real-time by measuring the average intensity change in a group of 4×4 pixels of the digitized hologram. The numerical reconstruction distance for each hologram was continuously updated. The final hologram reconstruction distance differs from the initial distance by about 40mm. Figure 1(a) shows clearly that the size of the reconstructed phase images, in terms of the pixel number, is reduced. This is as expected, since three holograms were recorded and reconstructed at different distances, namely d=100mm, d=117.3mm, and d=140.8mm.

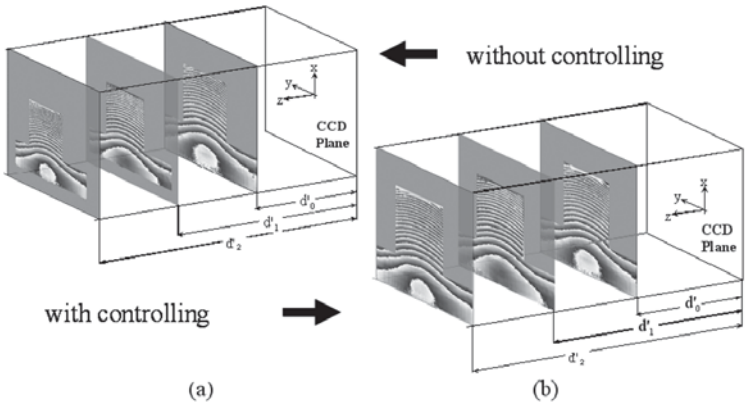

Figure 1. (a) In-focus phase map of the cantilever beam relative to three different reconstruction distances. (b) Wrapped image phases reconstructed at different distances after application of the zero-padding operation.

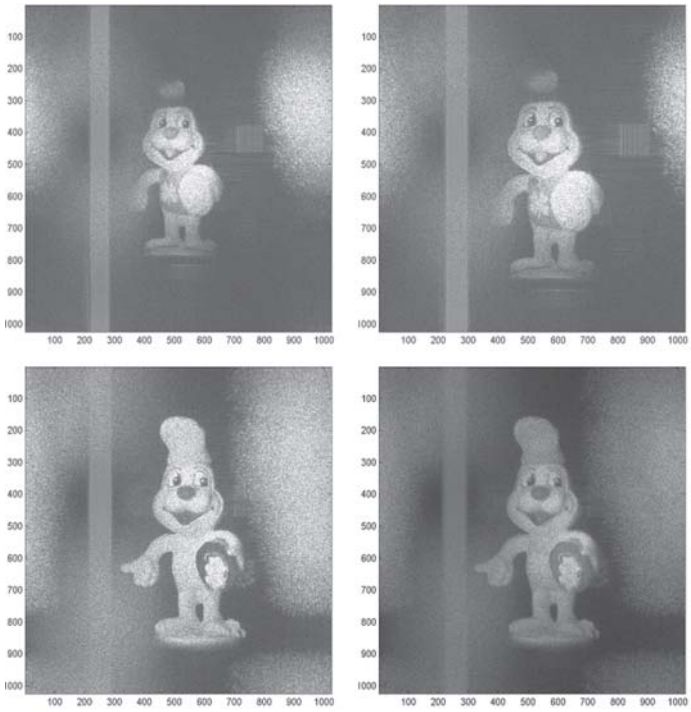

Figure 2. Reconstructed images from the digital hologram recorded at different wavelengths: (a) λ_1=632.8nm; (b) λ_2=532.0nm; λ_1=632.8nm, but size is controlled using the padding operation; superimposition of images (b) and (c).

The technique for controlling the size of the reconstructed images independently from a distance in order to permit a perfect superposition of both phase and amplitude images makes use of a larger number of pixels in the reconstruction process. This involves 'padding' with zeros so that the hologram recorded at the greater distance (d_2, with $d_2 > d_1$), is reconstructed with a number of pixels $N_2 = N_1(d_2/d_1)$ where N_1 is the number of pixels of the hologram recorded at wavelength λ_1. In this way, the same width for the RP is obtained, i.e., we have $\Delta x = \lambda_2 d/N_2\Delta\xi = \Delta x_1$. The values of the measured phase are restricted in the interval $[-\pi,\pi]$, i.e. they are wrapped. The wrapped image phases—reconstructed at different distances with application of padding operation—are shown in Figure 1(b).

We have also shown that the same approach can be usefully applied[6] in the case of multi-wavelength digital holography. The size of the RP can be kept constant, independent of wavelengths used during the recording process, by taking the hologram recorded at the greater wavelength and padding it with zeros. Figures 2(a) and (b) show the reconstructed amplitude images of a toy taken from two digital holograms. These were recorded using identical optical set-ups but with two different wavelengths (λ_1 = 632.8nm and λ_2 = 532.0nm, respectively). As is clearly seen, the image recorded in red appears to be smaller than that recorded in green. After padding, the reconstructed red hologram is shown in Figure 2(c). The two images (Figures 2(a) and (c)) are now the same size, can be superimposed to give a full-colour red and green image (shown in Figure 2(d)).

Continues on page 10.

Holographic visualization with digital micromirror devices

Today's computers and video rely on 2D perspective images to represent the physical world. As more holographic visualization methods are produced, users should increasingly see the advantage of true 3D and so spur the development of more applications. We are working on holographic visualization using the digital micromirror device (DMD). For our first applications, we envision pilot heads-up displays, air-traffic-control displays, and even ultrasound displays for medical diagnosis.[1-3] For those who don't know the device, the DMD is the micromechanical component of the Texas Instruments' Digital Light Processing (DLP) system.[3,4]

Applications are practical now because state-of-the-art DMD holograms can match the performance of competing 2D technologies: including in terms of resolution. The prototype holographic visualization system we are developing to demonstrate these applications may also be the forerunner to a DMD 'holovision' set. Our group has been investigating the projection of full-parallax holographic images using the DMD as the holographic medium.[5]

Initial applications using such displays can be achieved by showing virtual images of the hologram and can be developed into real-image projection displays using an additional component: a good volumetric display. Our group has had limited success in using frosted plates, screens, water mists, clouds, dry-ice vapor, and artificial fog as volumetric display devices.[5] By exploiting the translucent nature of Agarose gelatin in a glass tank, a relatively simple procedure, we have been able to project a good, undistorted volumetric image.[6]

Though low cost and simple, the gel is not durable and clearly not suitable for use on any aircraft. A gel-like display may be used for ultrasound, but the continuous scattering of light throughout the entire gel volume tends to fog the image.

As an alternative, we are developing a volumetric display system consisting of a series of liquid-crystal (LC) sheets and sequencing electronics.[6] The LC sheets are layered into a stack to form a cube that is placed in the location where the image is to form: the face of each LC sheet is perpendicular to the depth axis. Each sheet is a single liquid crystal 'pixel' about 16cm×16cm and one millimeter thick. All the sheets are normally on, causing minimum light scattering and attenuation. The sheets are sequenced at rates of 15Hz or faster to be free of flicker. As a LC sheet is sequenced *off*, it will cause the appropriate depth layer to form, making it appear brighter and sharper. Even with the number of LC sheet layers increased to approach a continuous medium, it still will not have the same continuous scattering problems as the Agarose gel since each opaque layer is only present a small fraction of the time. However, though is not as simple as the continuous medium, it is more durable, practical, and improves image quality.

Figure 1 is a picture of our prototype real-image holographic projection system. Its design is based on our laboratory setup, except the projection optical path is folded using flat surface mirrors.[5,6] The total projection path length is ~220cm and does not use any magnification. The size of the scene to be viewed is ~3.8cm: large enough for unaided viewing. The object scene is encoded for a 3.8×3.8×3.8cm^3 volume. Since there is no magnification, there should not be any nonlinearity in any direction in the projected image. All of the scene's depth cues will remain natural.[7]

Holographic 3D displays may potentially be used in all applications that currently use 2D perspective displays. The applications range from games to scientific workstations to holographic television. The prototype shown in Figure 1 is surely a step in the direction of a commercial holovision-set. Our near-term candidates for the DMD holographic 3D displays are those that do not need a 'live' image and can operate with current resolution levels. The projected images will be selected from a series of pre-recorded holograms: these could be computer generated or digitally recorded.

In heads-up display and air-traffic control applications, there is only a single viewer who does not need full color images or a wide look-around capability. A single-color laser and single DMD will thus suffice for the initial design of the device.

For medical ultrasound displays, the resolution of the current DMD exceeds the measurement resolution of the ultrasonic probe. But current ultrasound 2D displays have false color to enhance the image and use 2D perspective to appear to have a look-around. Until DMDs are produced with smaller mirrors, five or more DMDs may be necessary to project the image with sufficient look-around. The way this works is that holograms from different angles of the ultrasound 3D image are placed on different DMDs. As the viewer moves outside the viewing angle of one DMD, he move seamlessly into the next: in total, this will provide a 9° or better look-around of the object. The use of two different-colored lasers should

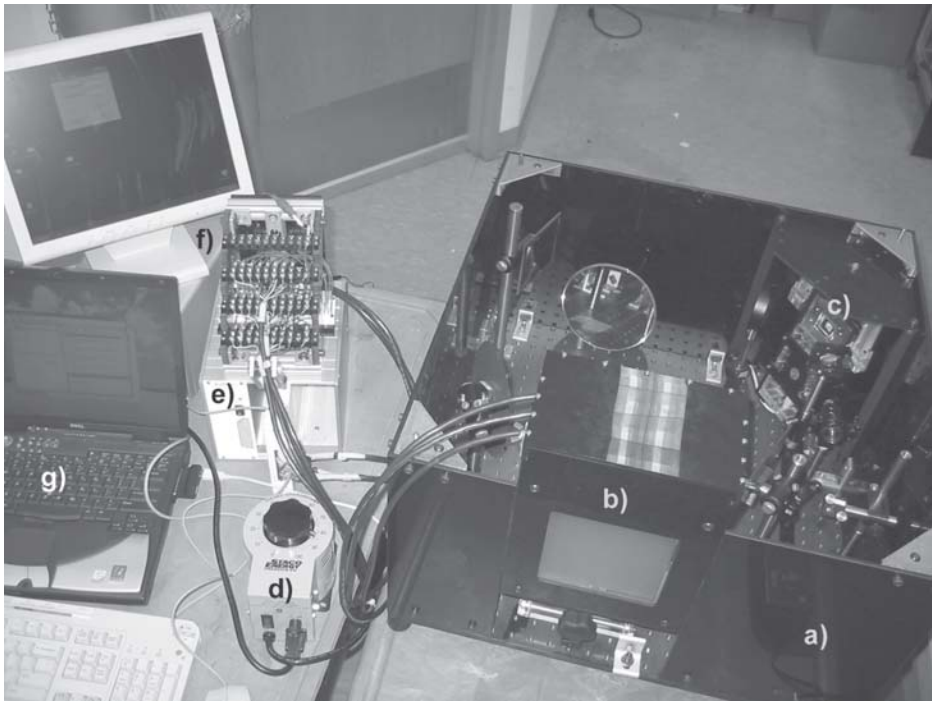

Figure 1. Major components of the prototype real-image holographic projection system: a) holographic projector housing; b) 24-liquid-crystal volumetric display; c) digital micromirror device (DMD); d) VAC Power Supply; e) NI SCXI-1128 Multiplexer Switch; f) computer for switching; and, g) computer to play holographic movies.

provide enough false color variation to match today's ultrasound. The choice of colors would be picked to match the users' needs.

As the work progresses, we are looking into commercializing the technology through licensing and by forming a company (Holomedix, Inc.) to develop applications. More information and images of our research are available on our web site.[8]

**Michael L. Huebschman,*
Bala Munjuluri,* Jeremy Hunt,
and Harold R. Garner*†**
Eugene McDermott Center for Human Growth and Development
*Center for Biomedical Inventions
†Department of Biochemistry and Department of Internal Medicine
The University of Texas Southwestern Medical Center at Dallas, TX
E-mail:
Michael.huebschman@utsouthwestern.edu

References

1. M. L. Huebschman, B. Munjuluri, and H. R. Garner, *Digital micromirrors enable holographic video display,* **Laser Focus World,** pp. 111-113, May 2004.
2. J. R. Thayn, J. Ghrayeb, and D. G. Hopper, *3-D display design concept for cockpit and mission crewstations,* **Proc. SPIE 3690,** pp. 180-185, 1999.
3. D. Dudley, *Micromirror Technology Enables More Than Projectors,* **Photonics Spectra,** pp. 76-78, May 2004.
4. D. Dudley, D. Duncan, and J. Slaughter, *Emerging Digital Micromirror Device (DMD) Applications,* **Proc. SPIE 4985,** pp. 14-25, 2003.
5. M. L. Huebschman, B. Munjuluri, and H. R. Garner, *Dynamic Holographic 3-D Image Projection,* **Optics Express 11** (5), pp. 437-445, 2003.
6. M. L. Huebschman, B. Munjuluri, J. Hunt, and H. R. Garner, *Holographic video display using digital micromirrors,* **Proc. SPIE 5742,** San Jose, CA, January 2005.
7. M. T. Stickland, S. McKay, and T. J. Scanlon, *The development of a three dimensional imaging system and its application in computer aided design workstations,* **Mechatronics 13,** pp. 521-532, 2003.
8. M. L. Huebschman, B. Munjuluri, and H. R. Garner, *NUVIEW:Dynamic Display of Real and Virtual 3-D Holographic Images Using TI's DMD,* http://innovation.swmed.edu/research/instrumentation/res_inst_dev3d.html.

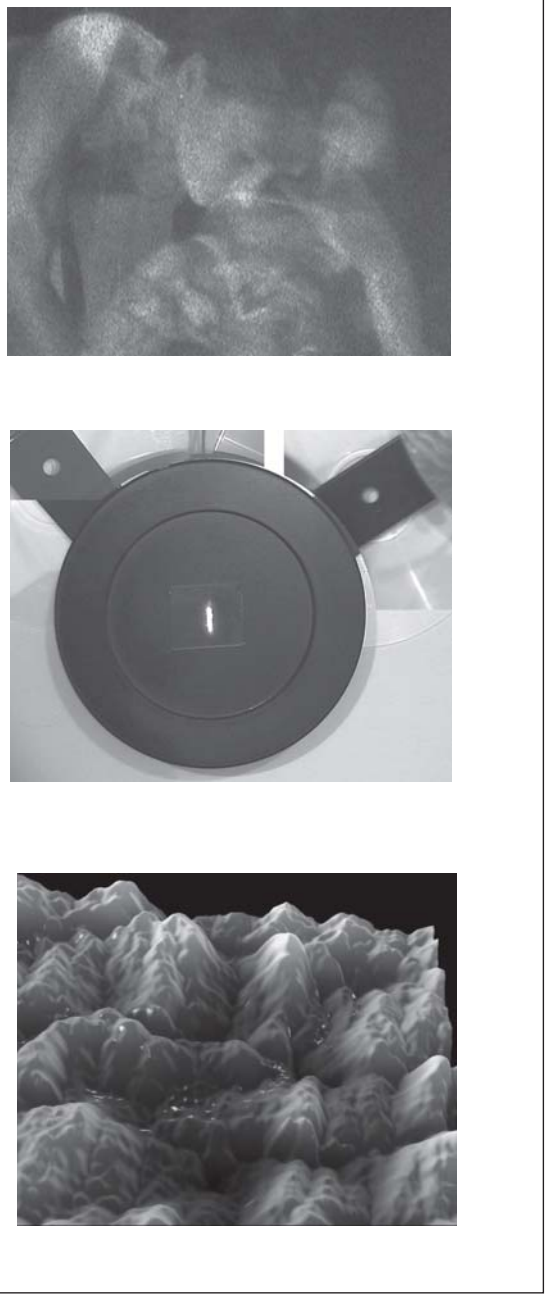

Figure 1. One object, several realities. Three pictures of the same object: the holographic reconstruction Narcissi *(left), the macroscopic hologram and reconstructing beam (center), and the structure of the hologram at the nano scale. Imagine them all in one.* Dietmar Öhlmann, MA(RCA) Braunschweig, Madamenweg, Germany. http://www.artBridge.info.

CROP photopolymer holographic storage media achieves archival data life times at areal density of greater than 100 bits/μm^2

Aprilis™ HMC and HMD photopolymerizable holographic recording material, in 400μm-thickness for card and disk optical media, was developed from ULSH-500 photopolymer systems. These exploited the method of cationic ring-opening polymerization (CROP)[1] for volume hologram recording. The CROP mechanism was used to replace free-radical polymerization and thereby achieved the lowest shrinkage[2,3] per unit reaction and high dynamic range,[4] while also achieving high recording sensitivity.[4,5] Sensitivity normalized to thickness, S_R, in cm/mJ was shown to be in the range $1 \le S_R \ge 12$ for multiplexed plane-wave holograms recorded in media thickness of 50 to 200μm. For binary data pages[6,7] multiplexed co-locationally in a thickness of 400μm, $0.33 \le S_R \le 6.75$. This corresponds to the typical recording manifold for attaining 90% of the cumulative dynamic range.

These advantageous recording sensitivities differentiate Aprilis™ media from others for data pages, as it means they can be recorded using pulsed lasers while the media is rotating. Good Bragg selectivity characteristics—consistent with uniform refractive-index modulation for the imaged thickness—was demonstrated for the CROP recording material.[2-7] The Bragg selectivity and the diffraction efficiency of recorded holograms are stable without requiring post-imaging fixing procedures.[2-7]

Data page holograms of low diffraction efficiency—such as $\eta \le 0.1\%$—are of particular interest for optical data storage. This is because it is desirable to multiplex, either co-locationally or through spatial overlapping, as many holograms as possible to maximize storage density and capacity. The theoretical upper limit on storage density is V/λ^3, where V is the volume of the hologram and λ is the wavelength of the light:[8] this is of the order of 10^{12}bits/cm^3. The limit not been achieved in practical systems due to limitations on signal-to-noise (SNR) relating to inter-page crosstalk between M multiplexed holograms and the diffraction efficiency having $1/M^2$ dependence. Grating strength scales with the thickness of the recording material,[9] but storage density is affected by geometrical contraints[10-12] associated with Bragg selectivity and the beam size, shape, and geometry.

For a typical off-axis reference-beam geometry, the area that is illuminated by the reference increases with both thickness, L, and inter-beam angle. Consequently, the excess area needed for the reference to overlap the signal beam is exacerbated with increased thickness. Furthermore, in photopolymer materials it is generally more difficult to record holograms of such low diffraction efficiency that exhibit good Bragg selectivity characteristics as the thickness is increased. Departure from an ideal sinc-squared function has been exhibited in thick photopolymer materials, which may be caused by non-uniformity of the recorded gratings through the thickness in the material.

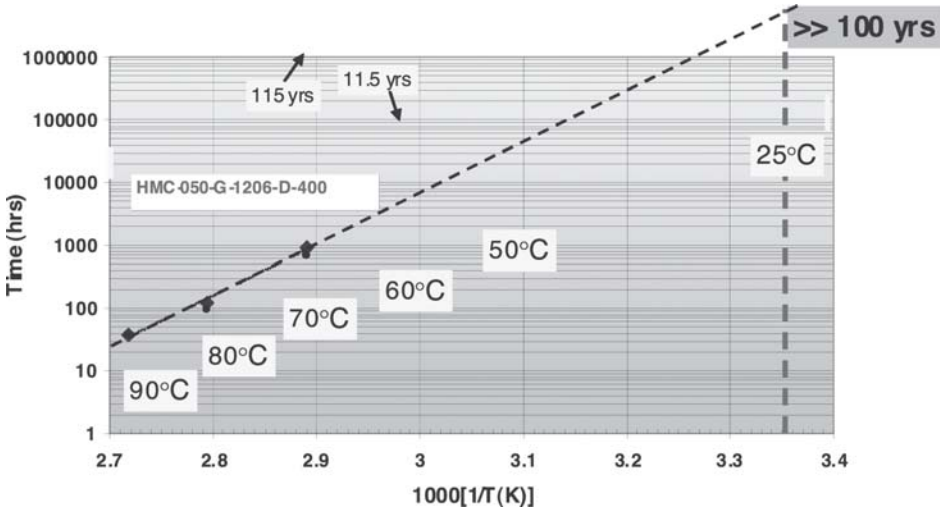

Figure 1. Plot for number of hours of persistent acceptable RBER (diamonds) and absorbance (circles) versus 1/T in K for storage of data page holograms at 73°C, 85°C and 95°C with applied linear-regression fit.

Critically-important attributes of a high-performance holographic material are that the material exhibit high dynamic range with good recording sensitivity. This allows high storage density without the need for a thick material that imposes limits due to the aforementioned factors. Additionally, the recorded information exhibits good fidelity that is reliably stable and thus archival. With an Aprilis™ HMC medium just 400μm thick,[6,7] storage density (S_{2D}) in the range of 100-150Gbits/in^2 was achieved for digital data. The information was recorded holographically as 262kbit pages with a dynamic range, $v_m = \sum \eta_i^{0.5}$, of at least M/# = 18. The stability of the signal-to-noise (SNR) and raw-bit-error-rate (RBER) of multiplexed data pages in Aprilis CROP materials due to large amounts of post-recording exposure energy and/or elevated temperatures has been established.[13] We discuss these issues here.

Experimental

The object beam optics comprise a 4f optical configuration using a custom matched Fourier-transform lens pair. The reference beam optics also comprise a 4f configuration. The laser, a Lightwave Model 142 CW DPSS Nd:YAG laser at 532nm, is spatially filtered and collimated to produce the object and reference beams. The azimuthal rotation angles of the sample plane about the optical axis (*z*-axis), φ, and the angle of the reference beam, θ, were controlled as previously described.[6] A Newport Model ESP-6000 Unidrive six-axis motion controller is used to position the sample, the takeoff mirror of the reference beam system, and the position of the CCD imager. Reconstruction of co-locationally-multiplexed digital-page holograms onto the CCD detector was accomplished using the reference beam with an incident intensity of 2.6m–5.6 W/cm^2, over the range of high to low θ, respectively. The increment of $\Delta\theta$ for planar-angle multiplexing exceeded the angular width requirements for peak-to-second-null of the Bragg selectivity. On the other hand, the increment of $\Delta\varphi$ for azimuthal multiplexing was about the requirement of peak-to-first-null for angular separation.

Frame grabbing of the reconstructed digital data pages from the Kodak CCD camera is accomplished with a National Instruments card rated up to 200MBytes/sec. An absolute error count for each data page is obtained from an error map that is determined for the entire reconstructed data page. A real-time histogram for the binning of detected 1s and 0s is determined and used in the alignment process during reading. A threshold

process for 0 and 1 level of grey scale is implemented for more accurate determination of the histogram representation, the process based upon using tile averaging[3,14-15] and control of gain. Real-time determination of raw BER for both thresholded and non-thresholded reads is used for the feedback loop to align the CCD camera, the imaging lens, the sample, and rotational positions for θ and φ. Final RBER is determined from the absolute pixel error count for each aligned data page.

Results and discussion

Peristrophic and planar-angle multiplexing of digital 512^2 (262kbit) data pages was carried out in 400μm-thick recording material of Aprilis™ HMD-050-G-D holographic media. This method of recording is advantageous in reducing inter-page cross talk and is effective for increasing the accessible angular bandwidth and thereby increasing areal density.[6-7,16-17] The area of the recording spot was determined as reported previously.[6] Storage density, S_{2D}, in excess of 100bits/μm^2 was achieved by using a range of rotational positions for φ over a full 2π. The average RBER was typically about 5.5E-4, with a number of data pages exhibiting values as low as 6E-5 to 7E-5, for recording where S_{2D}~100bits/μm^2.

The RBER was stable when the multiplexed data pages were subjected to extensive post-recording exposure at λ= 532nm corresponding to greater than 6000J/cm^2, a value that would be in excess of a billion read events. Samples comprising M=384 co-locationally-multiplexed plane-wave holograms, as well as M=100 co-locational binary-data-page holograms per storage location, were placed in ovens and held isothermally at temperatures of 73°C, 85°C, and 95°C for accelerated aging testing.

A number of optical and physical properties of the samples were evaluated periodically at room temperature as a function of storage time at the elevated temperatures. These included changes to cumulative grating strength, Bragg detuning and selectivity, volume scatter, absorbance, uniformity of physical structure, etc., as well as the RBER. Measured changes in the aforementioned properties and their inter-dependance were used to apply the classical Arrhenius method so as to make projections on archival lifetime of data stored at room temperature. For instance, an increase in visible absorbance by 13% from the value at the as-recorded state was set as a conservative estimate of the acceptable change for this property. Although this value can clearly be further relaxed as an independent property, it also effects other properties such as SNR of recorded digital data pages. An increase in the as-recorded average RBER of multplexed digital data pages to values in the range of 7E-3 to 9E-3, a value that is still readily correctable with standard low-overhead error correction codes, was similarly set as a conservative estimate of a reasonably acceptable change in RBER.

The Bragg selectivity profiles of both the plane-wave and digital data-page holograms exhibited slight increases in measured intensity near the first minima, and also some asymmetry in the intensities of the first subsidiary maxima (+/-) due to the accelerated aging, but the detuning angle remained constant to within about 0.01°. An unexpected result was that the cumulative grating strength, ν_m, was not only stable, but also increased by at least 20 to 25%. This was true for both the co-locational multiplexed plane-wave and digital-data-page holograms, when the stored information was subjected to accelerated aging at temperatures of 73°C, 85°C, and 95°C. This result distinguishes the Aprilis photopolymer material from others used in data-page recording, as they exhibit significant diminution in grating strength when subjected to elevated temperatures.

Figure 1 shows a linear-log plot of the storage temperatures in K versus averaged hours for persistent acceptable results for absorbance and for RBER (symbols are overlapping). The dotted line represents a linear regression that indicates that room-temperature storage of the recorded information is projected to be archival for substantially longer than 100 years. Furthermore, the physical attributes of the media exhibit no evidence of failure modes—such as due to locations of microcracks or de-lamination from substrates—even at temperatures in excess of 100°C.

D. A. Waldman, C. Wang, E. S. Kolb, and R. A. Minns
Aprilis, Inc
Maynard, MA
E-mail: waldman@aprilisinc.com

References

1. D. A. Waldman, R. T. Ingwall, P. K. Dhal, M. G. Horner, E. S. Kolb, H.-Y. S. Li, R. A. Minns, and H. G. Schild, *Diffractive and Holographic Optics Technology III,* **Proc. SPIE 2689** (15), pp. 127-141, 1996.
2. D. A. Waldman, H.-Y. S. Li, and M. G. Horner, *Volume shrinkage in slant fringe gratings of a cationic ring-opening holographic recording material,* **J. Imag. Sci. Technol. 41** (5), pp. 497-514, 1997.
3. R. M. Shelby, D. A. Waldman, and R. T. Ingwall, *Distortions in pixel-matched holographic data storage due to lateral dimension change of photopolymer storage media,* **Opt. Lett. 25** (10), p. 713, 2000.
4. D. A. Waldman, H.-Y.S. Li, and E. A. Cetin, *Holographic Recording Properties in Thick Films of ULSH-500 Photopolymer,* **Proc. SPIE 3291,** pp. 89-103, 1998.
5. R. T. Ingwall and D. A. Waldman, *Photopolymer Systems,* **Holographic Data Storage,** H. J. Coufal, D. Psaltis and G. T. Sincerbox, (Eds.), pp. 171-197, Springer-Verlag, New York, 2000.
6. D. A. Waldman, C. J. Butler, and D. H. Raguin, *CROP holographic storage media for optical data storage at greater than 100 bits/μm^2,* **Proc. SPIE 5216,** pp. 10-25, 2003.
7. D. A. Waldman, *Recent developments in Aprilis high capacity CROP photopolymer media,* **Proc. SPIE 5521,** pp. 5521-5531, 2004.
8. P. J. Van Heerden, *Theory of optical information storage in solids,* **Appl. Opt. 2,** pp. 393-400, 1963.
9. H. Kogelnik, *Coupled Wave Theory For Thick Hologram Gratings,* **Bell Sys. Tech. J. 48,** p. 2909, 1969.
10. H.-Y. S. Li and D. Psaltis, *Three dimensional holographic disks,* **Appl. Opt. 33** (17), pp. 3764-3774, 1994.
11. G. J. Steckman, A. Pu, and D. Psaltis, *Storage density of shift-multiplexed holographic memory,* **Appl. Opt. 40** (20), pp. 3387-3394, 2001.
12. G. Barbastathis, M. Levene, and D. Psaltis, *Shift multiplexing with spherical reference waves,* **Appl. Opt. 35** (14), pp. 2403-2417, 1996.
13. D. A. Waldman, C. Wang, E. S. Kolb, C. J. Butler, and D. H. Raguin, *Holographic data storage - Photopolymer material and drive technology,* **Proc. OSA Annual Meeting - DOMO,** October 2004.
14. G. W. Burr, J. Ashley, H. Coufal, R. K. Grygier, J. A. Hoffnagle, C. M. Jefferson, and B. Marcus, *Modulation coding for pixel-matched holographic data storage,* **Opt. Lett. 22** (19), pp. 639-641, 1997.
15. R. M. Shelby, J. A. Hoffnagle, G. W. Burr, C. M. Jefferson, M.-P. Bernal, H. Coufal, R. K. Grygier, H. Günther, M. McFarlane, and G. T. Sincerbox, *Pixel-matched holographic data storage with megabit pages,* **Opt. Lett. 22** (19), pp. 1509-1511, 1997.
16. K. Curtis, A. Pu, and D. Psaltis, *Method for holographic storage using peristrophic multiplexing,* **Opt. Lett. 19** (13), pp. 993-994, 1994.
17. A. Pu and D. Psaltis, *High-density recording in photopolymer-based holographic three-dimensional disks,* **Appl. Opt. 35** (14), pp. 2389-2398, 1996.

Calendar

2005

Optics & Photonics
31 July - 4 August
San Diego, California USA
co-located with the SPIE 50th Annual Meeting: Celebrating 50 Years of Excellence
Program • Advance Registration Ends 15 July 2005
Exhibition
spie.org/conferences/programs/05/am/

Seventh International Conference on Correlation Optics
6 - 9 September
Chernivtsi, Ukraine
Sponsored by SPIE Ukraine Chapter and SPIE Russia Chapter.
SPIE will publish proceedings.
spie.org

SPIE Europe Symposium Optics/Photonics for Defence & Security
26 - 29 September
Bruges, Belgium
Call for Papers • Abstracts Due 11 April 2005
Exhibition
spie.org/conferences/calls/05/eud/

2006

IS&T/SPIE's Electronic Imaging 2006
15 - 19 January 2006
San Jose, California USA
Call for Papers • Abstracts Due 5 July 2005
electronicimaging.org/Call/06/

New software tools facilitate the development of better holographic systems

The effective development of new holographic systems requires a careful understanding of the set-up under consideration. In particular, the precise arrangement of hologram geometry and optical components involved can dramatically alter the performance of a holographic system down to the microscopic level. In addition, unlike many optical-design endeavors, each holographic system is typically custom designed and constructed from scratch. As such, it is usually not possible to follow a prescribed optical layout in advance. By their nature, holographic systems place very different demands on optical modeling software than more traditional applications, such as lens design. In particular, it is often more important to obtain an intuitive understanding of how the system operates than it is necessary to calculate the 'optimal' configuration. As such, traditional lens-design software packages are not always well suited for holographic system development.

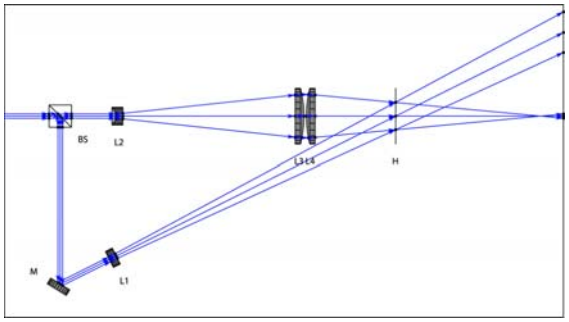

Figure 1. Recording geometry schematic of a holographic optical element as modeled and rendered by Rayica.

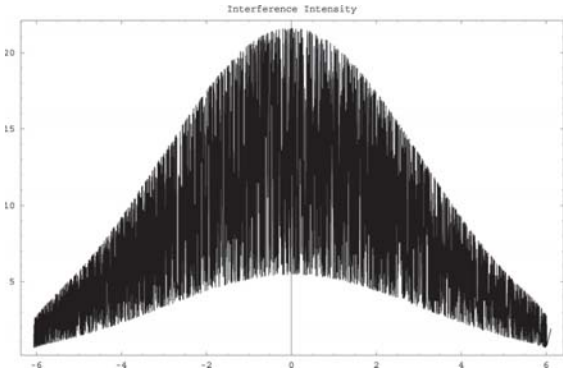

Figure 2. Modulation depth of the interference fringes at the hologram plane calculated by Wavica. *Horizontal scale: millimeters. Vertical scale: relative intensity.*

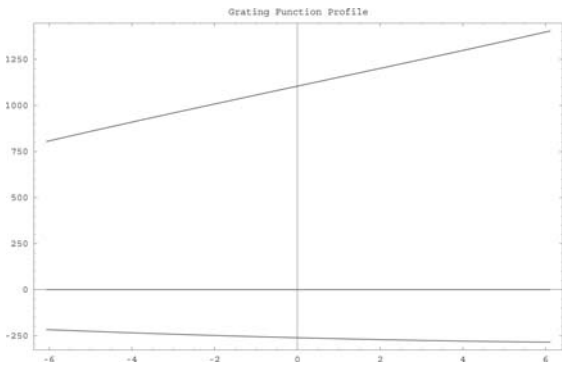

Figure 3. Recorded grating-vector profile calculated by Wavica *(vertical axis is in inverse millimeters, horizontal axis is in millimeters). The top curve shows the in-plane frequency component and the bottom curve the out-of-plane frequency component.*

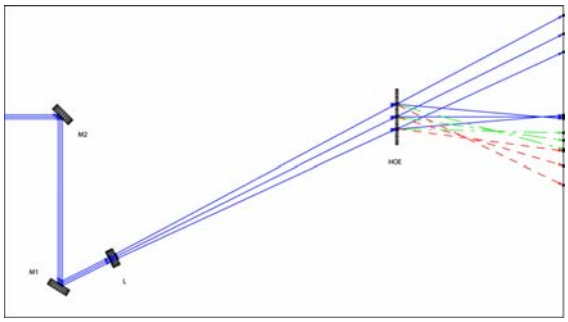

Figure 4. Diffractive behavior of the constructed holographic element at the three different wavelengths: 405nm (solid line), 532nm (dash-dot line), and 660nm (dashed line). Here, the HOE grating function was determined by Wavica, *and the resulting holographic reconstruction was traced by* Rayica.

My secret weapon

Throughout my brief twenty-year career as a scientist and engineer, I have maintained a secret weapon in my development of new holographic systems. This weapon is my own personal optical modeling software. In particular, for me, holographic research and the development of this software have always gone hand-in-hand. This joint development effort resulted in the release of my commercial optical-design package, *Optica*, in 1994. Written in the *Mathematica* language, *Optica* is slower in execution than other optical-design software packages written in C or Fortran. Nevertheless, I have found the leverage obtained from *Mathematica*'s symbolic and computational powers has more than compensated for its relative slowness.

Since its first release ten years ago, *Optica* has sold more than 2,000 copies worldwide, and I have continued to expand its functionality. Recently, my efforts have resulted in two new commercial optical modeling packages—called *Rayica* and *Wavica*—that now replace the original *Optica* package. These software offerings are distributed by my company, Optica Software.

Rayica and *Wavica* work seamlessly within the *Mathematica* environment. They extend the *Mathematica* language for describing and modeling the behavior of optical systems. *Rayica* is responsible for performing geometric, non-sequential, polarization ray-trace calculations of optical systems in three-dimensional space. *Wavica* builds on the functionality of *Rayica* and *Mathematica* to calculate wave-front interference and diffraction, Gaussian-beam propagation, ABCD matrix models, and analytic representations of optical systems. In addition to modeling optical systems, *Rayica* and *Wavica* also produce high-quality graphics suitable for publication in research reports, grant proposals, and patent applications.

Modeling a holographic system

Next, lets examine a holographic system modeled with *Rayica* and *Wavica*. Figure 1 shows a schematic, generated by *Rayica*, that exhibits an optical geometry used to record a holographic optical element. Here, the precise scale and behavior of every optical component is accurately calculated and depicted. In particular, a Gaussian laser beam (wavelength 405nm) is shown directed into a beam-splitter cube (BS). This splits the beam into the diverging off-axis reference pathway (given by the mirror, M, and the first lens, L1) and the converging on-axis object pathway (given by L2, L2, and L4) that finally interfere at the holographic plate H. After *Rayica* has modeled the optical layout, *Wavica* is used to examine the modulated interference fringes during recording (Figure 2) and the resulting diffraction-grating vector function after development of the hologram (Figure 3).

Finally, the resulting grating structure from *Wavica* is used by *Rayica* to model the holographic reconstruction for different wavelengths, shown in Figure 4. Although not shown, *Rayica* can also model different illumination geometries with the same hologram.

Holographic imaging in the presence of aberrations

There are some applications of holographic imaging where intrinsic aberrations (due to reconstruction wavelength shifts or the presence of curved optical windows) can potentially dominate the information content and cripple the intended holographic measurement. It then becomes necessary to compensate for the aberrations in some way. In such instances, accurate characterization of the aberrations becomes an essential component of the overall optical system design. In particular, optical modeling software, such as *Rayica* and *Wavica*, can be used to model the aberrations and design the necessary corrective optics. Additional examples of modeling holographic systems with *Rayica* and *Wavica* can viewed on our website.

Conclusion

Although originally developed for my own holographic research, I have found that the broad requirements of holographic systems modeling have enabled the applicability of *Rayica* and *Wavica* to numerous other optical modeling projects. In fact, today, most of my users have nothing to do with holographic research and the true origin of my software development efforts is largely unrecognized. Nevertheless, my software continues to remain a potent weapon in my personal arsenal for holographic research.

Donald Barnhart
Lead Developer
Optica Software Division of iCyt Mission Technology, Inc.
Champaign, IL
E-mail: donald@opticasoftware.com
http://www.opticasoftware.com

Combining optical holograms with interactive computer graphics

Continued from cover.

they can serve as optical combiners and produce very compact displays. Real-time (stereoscopic or autostereoscopic) computer graphics can be integrated into the hologram on one side, while illuminating it partially from the other.

Rendering and illumination are view-dependent and therefore must be synchronized. If autostereoscopic displays are used to render the 3D graphics registered to the hologram, both holographic and graphical content appear three-dimensional within the same space. If the depth information is known for both, the correct occlusion effects between the hologram and graphics can be generated.

Figure 1 shows a rainbow hologram of a dinosaur skull combined with graphical representations of soft tissue and bones. If the holographic plate is illuminated with a uniform light, the entire hologram is reconstructed (Figure 1, left). If the plate is illuminated only at the areas not occluded by graphical elements, the synthetic objects can be integrated by displaying them on the screen behind the plate (Figure 1, right).

The reconstructed object wave amplitude is proportional to the reference wave intensity. In addition to using an incomplete reference to reconstruct a fraction of the hologram, intensity variations in the projected light allow local modification of the recorded object-wave amplitude.

Practically, this means that—to create the illumination image sent out by the projector—graphical shading and shadowing techniques are used to reconstruct the hologram instead of illuminating it with uniform intensity. To do this, we must neutralize both the real shading effects in the captured scenery—caused by the real light sources used for illumination during hologram recording—and the physical lighting effects caused by the video projector on the holographic plate. Next, we must simulate the influence of a synthetic illumination.[1]

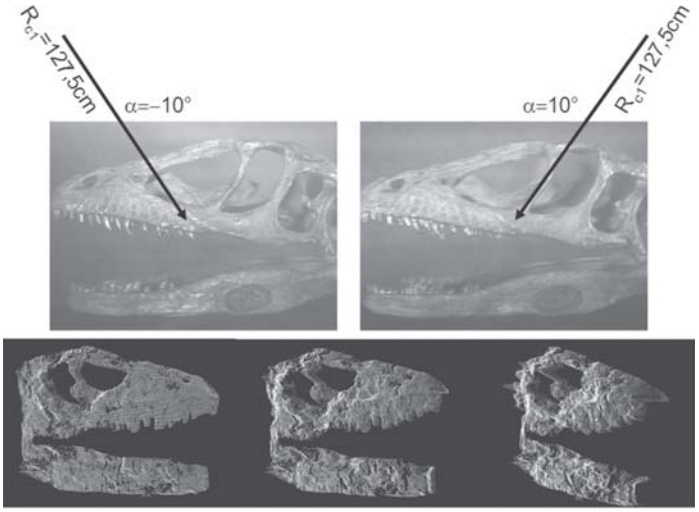

Figure 3. Two scans of a rainbow hologram with different reference wave angles (top), and point-cloud of reconstructed depth map (bottom).

Using conventional graphics hardware, it becomes possible not only to create consistent shading effects, but also to cast synthetic shadows correctly from all holographic and graphical elements onto all other elements.

Figure 2 shows the same rainbow hologram as above with 3D graphical elements and synthetic shading effects. Shadows are cast correctly from the hologram onto the graphics and vice versa. A virtual point-source of light was first located at the top-left corner (L_1 in Figure 2, left) and then moved to the top-right corner (L_2 in Figure 2, right) in front of the display. Moving the virtual light source and computing new shading effects can be done in real-time. Note that only intensity/shading variations are simulated in Figure 2. A vertical variation of the object beam wavelength, due to diffraction effects from the rainbow hologram, is still visible and cannot be corrected. This is not the case for white-light reflection holograms.

Depth information of the recorded holographic content is essential for a correct rendering. The shading and occlusion effects described above would not be possible without knowing the surface geometry of the holographic content. The depth information can be estimated using commercial flatbed scanners. They can be used to scan multiple images of a hologram by placing the holographic film on top of the scanner window, leaving the lid open, and illuminating from different angles for each scan (cf. Figure 3, top). The geometric image distortion that is caused by the different illuminations[2] is captured in these images. An analytical solution exists for computing depth information if the correspondences between 2D image projections (disparities) are known: this is shown in Figure 3, bottom.

Oliver Bimber
Bauhaus University
Weimar, Germany
E-mail:
oliver.bimber@medien.uni-weimar.de
http://www.holographics.de

References

1. O. Bimber, *Combining Optical Holograms with Interactive Computer Graphics*, **IEEE Computer,** pp. 85-91, January 2004.
2. E. B. Champagne, *Nonparaxial Imaging, Magnification, and Aberration Properties in Holography*, **J. of the Optical Society of America 57** (1), pp. 51-54, 1967.

An update on silver halide holographic materials

Continued from page 2.

Material / Manufacturer	Optimal exposure (μJ/cm2)	Peak diffraction efficiency	Peak bandwidth (nm)	Shrinkage	Typical absorption
BB / Colourholographic	150	77.7%	34	-2.4%	13%
PFG-3C / GEOLA	2000	80.7%	24	+1.1%	20%
PFG-01 / GEOLA	300	55.4%	22	-3.5%	15%
Ultimate-15 / Gentet	150	82.6%	40	+0.3%	16%
Ultimate-08 / Gentet	400	78.0%	35	-1.0%	16%

is applied. This is essential for the production of holographic reflection masters. Second, if scattering is a critical issue, the BB-materials are superior to the other emulsions. However, while a slight over-exposure of this material may help to decrease absorption and scattering even more, too much deposited energy causes the diffraction efficiency to drop significantly. Finally, for pure display purposes, the Ultimate materials are probably the best choice: they provide a large reconstruction bandwidth and high peak diffraction efficiency in all wavelength regions.

We hope that these curves suggest the adequate exposure range and that the data provided in this article helps fellow holographers to choose the holographic emulsion that best fits their application.

M. Schmiedchen, J. Hanf, W. V. Spiegel, and T. Tschudi
Institute of Applied Physics
Darmstadt University of Technology, Germany
E-mail: marc.schmiedchen@physik.tu-darmstadt.de

References

1. Y. Gentet and P. Gentet, *ULTIMATE emulsion and its applications: a laboratory made silver-halide emulsion of optimized quality for monochromatic, pulsed and full color holography,* **Proc. SPIE 4149,** pp. 56-62, 2000.
2. UAB GEOLA, *Emulsions for Holography,* **Technical Product Specifications And Sales Information Brochure**, 2001.
3. H. I. Bjelkhagen, T. H. Jeong, and D. Vukicevic, *Color reflection holograms recorded in a panchromatic ultrahigh-resolution single layer silver-halide emulsion*, **J. Imaging Sci. Technol. 40,** pp. 134-146, 1996.
4. H. I. Bjelkhagen, *Commercial silver-halide materials,* **Silver-Halide Recording Materials**, pp. 93-113, Springer, Berlin, 1997.
5. M. Ulibarrena and R. Madrigal, *Current BB640 color plates compared to HRT's,* **SPIE Holography newsletter 12** (2), p. 9, 2001.
6. H. I. Bjelkhagen, *An update on commercial recording materials,* **SPIE Holography newsletter 13** (2), p. 2, 2002.

Machine vision for defect detection on silicon wafers

Continued from page 12.

Fabrice Meriaudeau, Pierrick Bourgeat[*], Patrick Gorria, and Kenneth Tobin[†]
Le2i Laboratory
University of Burgundy, France
[*]BioMedIA Laboratory
CSIRO, Australia
[†]Oak Ridge National Laboratory, TN
E-mail: f.meriaudeau@iutlecreusot.u-bourgogne.fr

References

1. C. E. Thomas Jr., et al. *Direct to digital holography for high aspect ratio inspection of semiconductor wafers,* **2003 Int'l Conf. on Characterization and Metrology for ULSI Technology, Proc. AIP Vol. 683**, pp. 254-270, Austin, March 2003.
2. P. Bourgeat, F. Meriaudeau, P. Gorria, and K. W. Tobin, *Content-based segmentation of patterned wafer for automatic threshold determination,* **Proc. SPIE 5011,** pp. 183-189, 2003.
3. P. Bourgeat, F. Meriaudeau, K. W. Tobin, and P. Gorria, *Patterned wafer segmentation,* **Quality Control by Artificial Vision, Proc. SPIE 5132**, pp. 36-44, 2003.
4. P. Bourgeat, **Segmentation d'images de semi-conducteurs appliquée à la détection de défauts,** Ph.D. thesis, Université de Bourgogne, 2004.
5. P. Bourgeat, F. Meriaudeau, K. W. Tobin, and P. Gorria, *Features extraction on Complex images,* **Proc. OSAV'2004, Int. Topical Meeting on Optical Sensing and Artificial Vision**, pp. 103-110, Saint Petersburg, Russia, 18-21 October 2004.
6. F. Meriaudeau, P. Bourgeat, P. Gorria, and K. Tobin, *Classifier Combination on Features extracted From Complex images: Application to Defect Detection on Silicon Wafers,* **Proc. QCAV'05**, Japan, May 2005.

Controlling phase and amplitude image reconstructions in digital holography: achievements and perspectives

Continued from page 3.

S. De Nicola, A. Finizio, G. Pierattini, D. Alfieri[*], S. Grilli[*], L. Sansone[*], P. Ferraro[*], G. Coppola[†], and B. Javidi [††]
Institute of Cybernetics 'E. Caianiello' of the National Research Council (CNR), Pozzuoli, Italy.
[*]National Institute of Applied Optics
[†]Institute of Microelectronics and Microsystems of the CNR
[††]University of Connecticut
E-mail: p.ferraro@cib.na.cnr.it

References

1. D. Gabor, *A new microscopic principle,* **Nature 161,** p. 777, 1948.
2. J. W. Goodman and R.W. Lawrence, *Digital image formation from electronically detected holograms,* **Appl. Phys. Lett. 11,** p. 7, 1967.
3. U. Schnars, *Direct phase determination in hologram interferometry with use of digitally recorded holograms,* **J. Opt. Soc. Am. A. 11,** p. 2011, 1994.
4. P. Ferraro, S. De Nicola, A. Finizio, G. Coppola, D. Alfieri, L. Aiello, S. Grilli, and G. Pierattini, *Controlling several image parameters in the digital holographic reconstruction process,* **Proc. SPIE 5557,** p. 1, 2004.
5. P. Ferraro, G. Coppola, D. Alfieri, S. De Nicola, A. Finizio, and G. Pierattini, *Recent advancements in digital holographic microscopy and its applications,* **Proc. SPIE 5457,** p. 481, 2004.
6. B. Javidi, P. Ferrao, S-H. Hong, S. De Nicola, A. Finizio, D. Alfieri, and G. Pierattini, *Three-dimensional image fusion by use of multiwavelength digital holography,* **Opt. Lett. 30,** p. 144, 2005.

Join the Technical Group

...and receive this newsletter

Membership Application

Please Print ☐ Prof. ☐ Dr. ☐ Mr. ☐ Miss ☐ Mrs. ☐ Ms.

First Name, Middle Initial, Last Name _____

Position _____ SPIE Member Number _____

Business Affiliation _____

Dept./Bldg./Mail Stop/etc. _____

Street Address or P.O. Box _____

City/State _____ Zip/Postal Code _____ Country _____

Telephone _____ Telefax _____

E-mail Address/Network _____

Technical Group Membership fee is $30/year, or $15/year for full SPIE members.

❑ Holography
Total amount enclosed for Technical Group membership **$** _____

❑ **Check enclosed.** Payment in U.S. dollars (by draft on a U.S. bank, or international money order) is required. Do not send currency. Transfers from banks must include a copy of the transfer order.

❑ **Charge to my:** ❑ VISA ❑ MasterCard ❑ American Express ❑ Diners Club ❑ Discover

Account # _____ Expiration date _____

Signature _____
(required for credit card orders)

This newsletter is printed as a benefit of membership in the **Holography Technical Group.** Technical group membership allows you to communicate and network with colleagues worldwide.

Technical group member benefits include: a semi-annual copy of the *Holography* newsletter; SPIE's monthly publication, **oe***magazine;* and a membership directory.

SPIE members are invited to join for the reduced fee of $15. If you are not a member of SPIE, the annual membership fee of $30 will cover all technical group membership services. For complete information and a full application form, contact SPIE.

Send a copy of this form to:
SPIE • P.O. Box 10
Bellingham, WA 98227-0010 USA
Tel: +1 360 676 3290
Fax: +1 360 647 1445
E-mail: spie@spie.org
Anonymous FTP: spie.org

Please send me
☐ Information about full SPIE membership
☐ Information about other SPIE technical groups
☐ FREE technical publications catalog

Reference Code: 4646

HOLOGRAPHY ONLINE

Holography Web Discussion Forum

You are invited to participate in SPIE's online discussion forum on Holography. To post a message, log in to create a user account. For options see **"subscribe to this forum."**

You'll find our forums well-designed and easy to use, with many helpful features such as automated email notifications, easy-to-follow "threads," and searchability. There is a full FAQ for more details on how to use the forums.

Main link to the Holography forum:
http://spie.org/app/forums/tech/

Related questions or suggestions can be sent to **forums@spie.org.**

The International Society for Optical Engineering

Holography

This newsletter is published semi-annually by SPIE—The International Society for Optical Engineering, for its International Technical Group on Holography.

Editors and Technical Group Chairs Hans Bjelkhagen, Raymond Kostuk
Technical Editor Sunny Bains
Editorial Assistant Stuart Barr
Managing Editor Linda DeLano

Articles in this newsletter do not necessarily constitute endorsement or the opinions of the editors or SPIE. Advertising and copy are subject to acceptance by the editors.

SPIE is an international technical society dedicated to advancing engineering, scientific, and commercial applications of optical, photonic, imaging, electronic, and optoelectronic technologies. Its members are engineers, scientists, and users interested in the development and reduction to practice of these technologies. SPIE provides the means for communicating new developments and applications information to the engineering, scientific, and user communities through its publications, symposia, education programs, and online electronic information services.

SPIE—The International Society for Optical Engineering, P.O. Box 10, Bellingham, WA 98227-0010 USA. Tel: +1 360 676 3290. Fax: +1 360 647 1445.

European Office: Karin Burger, Manager, karin@spieeurope.org, Tel: +44 7974 214542. Fax: +44 29 2040 4873.

In Russia/FSU: 12, Mokhovaja str., 119019, Moscow, Russia. Tel/Fax: +7 095 202 1079. E-mail: edmund.spierus@relcom.ru

Machine vision for defect detection on silicon wafers

Silicon wafers are massively used in the semiconductor and microelectronics industries. With this material, it is of extreme importance to obtain a defect-free surface to improve yield and performance of the microchips. Current practice in the industry is to inspect the wafers for any surface defects only at the end of the final polishing stage. Techniques such as atomic force microscopy, scanning tunneling force microscopy, scanning electron microscopy, x-rays and acoustic electron microscopy have all been used to perform the surface-defect characterization. However, all these methods require cumbersome equipment that is expensive to use on a daily basis in a production factory.

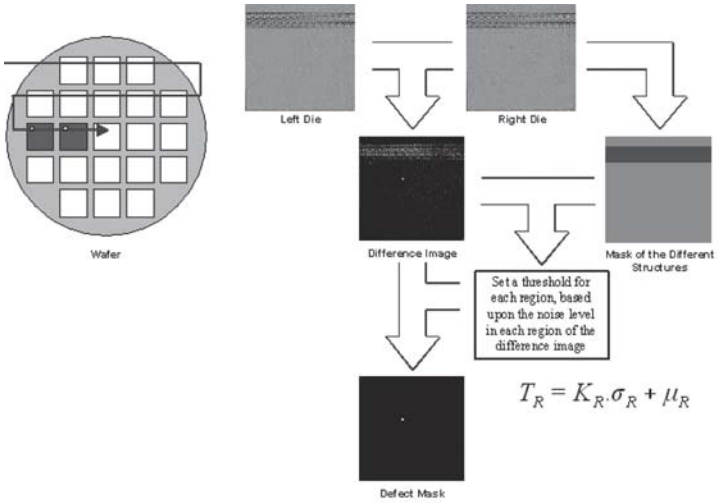

Figure 1. Principle of die-to-die wafer inspection and defect detection with the creation of a mask for local noise and threshold estimation. Respectively, μ and σ are the average grey and the standard deviation in the different regions.

We have developed an alternative technique that relies on the use on the direct-to-digital holography (DDH).[1] This allows us to capture the complex image of a scene, and then reconstruct the phase and amplitude information. This gives us a complete 3D representation of the scene within the wavelength depth of the laser used to produce the hologram: thus it provides a new dimension to texture analysis.[2,3]

In die-to-die wafer inspection (see Figure 1), defect detection is based on the comparison of the same area on two neighboring dies. Images being thoroughly aligned, the dissimilarities between the images are a result of defects in the area of one of the dies. The two images are subtracted, and a threshold level is selected to locate any anomaly.

To optimize the signal-to-noise ratio, the threshold value is established based upon the noise level in the difference image. However, since multiple structures coexist in the same field of view, the noise level can vary over a single image preventing the use of a global threshold. To overcome this problem, a segmentation is done to create a mask of the different regions (each region being a class for our classifier) in order to produce a measure of noise for each structure in the difference image. This leads to an individual threshold for each region (see Figure 1).

The mask is created through a 'classification-segmentation' procedure. The complex image provided by the DDH is first processed to generate four new images: the phase (P), normalized-amplitude (NA), and complex images (C); and also the complex image with normalized amplitude (CAN).[5] Each image is then filtered with a bank of Gabor filters (see Figure 2).

The processed images are then used as input in a vote SVM (support vector machine) classifier.[6]

A pixel is classified as pertaining to a given class (dynamic RAM, logic area, or blank area) if it is identified as such by at least two of the three best classifiers. A so-far unclassified pixel (a pixel identified as being part of a different class by each of the three classifiers) is classified according to the results of the fourth classifier. Figure 3 shows an example of a segmented image. The obtained results show robust segmentation.[4,6]

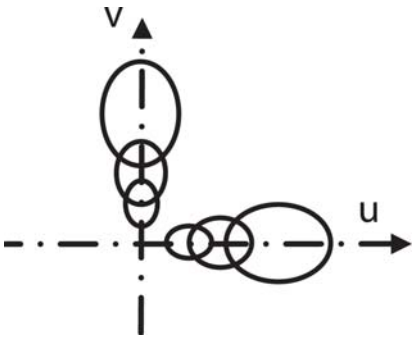

Figure 2. Bank of Gabor filters with three scales and two orientations.

Figure 3. Example of a segmented image.

The technique we developed enables us to train the classifier with a small set of examples and to obtain results similar to those produced using a full training set. The technique can be applied to any type of optical tool for wafer inspection, but in the particular case of the DDH, the extra information provided by the complex nature of the image makes it even more powerful. The classification has been applied to defect detection and led to a tremendous improvement in the final results:[4] the ratio of false detection to no detection.

Continues on page 10.

SPIE Society of Photo-Optical Instrumentation Engineers
P.O. Box 10 • Bellingham, WA 98227-0010 USA

Change Service Requested

DATED MATERIAL

Non-Profit Org.
U.S. Postage Paid
Society of
Photo-Optical
Instrumentation
Engineers